Magnetoresistance of nanocontacts with constrained magnetic domain walls

J.-E. Wegrowe,* T. Wade, X. Hoffer, L. Gravier, J.-M. Bonard, and J.-Ph. Ansermet
Institut de Physique Expérimentale, Ecole Polytechnique Fédérale de Lausanne, CH-1015 Lausanne, Switzerland
(Received 22 July 2002; published 20 March 2003)

Spin-dependent transport was studied in single contacted granular nanowires composed of carbon encapsulated magnetic nanoparticles embedded in a Co or permalloy matrix. A large variety of magnetoresistance (MR) signals were measured. The ratio of the maximum variation of the resistance as a function of the magnetic field over the minimum resistance $\Delta R/R_{\min}$ ranges from a few to 10 000 %. Characterization of the samples was performed, including hysteresis loops as a function of the amplitude and angle of the applied magnetic field, temperature, as well as *I-V* characteristics and relaxation time. The huge MR signals are probably associated with a reversible mechanical change of the structure of the matrix close to a conduction channel. When this huge magnetomechanical effect is avoided, a change of the transport regime is observed, and ballistic MR of some tens of percents can be measured.

DOI: 10.1103/PhysRevB.67.104418 PACS number(s): 75.60.Ch, 75.47.De, 72.15.Gd

I. INTRODUCTION

The study of the physical properties of nanocontacts is a key issue of spintronics.[1] At the nanoscopic scale, any contact is a junction characterized by the nature of the coupling to the reservoirs of energy, particles, charge, pressure, spin polarized electron, etc.[2] If the contact is ferromagnetic, or near a ferromagnetic layer, the spin polarization of the electrons plays an important role, and leads to the large variety of effects exploited in spintronics. The measurement of the resistance as a function of the magnetic field, i.e. the magnetoresistance, is intensively used to study the physical properties of junctions with well defined magnetic configurations. Well-known examples are tunnelling junctions giving rise to tunnelling magnetoresistance (TMR),[3–5] ferromagnetic/metal/ferromagnetic junctions giving rise to giant magnetoresistance (GMR),[6–9] or spin injection in semiconductor/ferromagnetic junctions. If the size of the contact is nanometric or subnanometric, a ballistic junction (BJ) is expected. In the presence of constrained magnetic domain walls at the scale of the junction,[10,11] a new type of magnetoresistance must then be considered, namely, ballistic magnetoresistance (BMR). Experimental works were published recently, all in form of letters.[12–15] Very large magnetoresistances were measured, of the order of some few 100%.

The motivation of the present work is to study ballistic junctions obtained by the method of electrodeposition of Co and permaloy ($Ni_{81}Fe_{19}$) matrix in nanoporous membrane templates, previously filled with cobalt magnetic nanoparticles[16] encapsulated by a carbon shell. Although only a single nanowire is contacted in the membrane, the sample is a circuit composed of many junctions.

Three different mechanisms can be invoked to describe the transport in our samples.

(I) Diffusive junctions (DJ), where the nanoparticles play the role of pinning centers of constrained magnetic domain walls. The transport is diffusive (see Ref. 16), and GMR-like magnetoresistance is expected.

(II) Tunnelling junctions (TJ). The Co or permaloy matrix plays the role of leads. Two scenarii are then possible: either the carbon shell of the nanoparticles plays the role of isolating junctions or a small bridge or a hole in the Co or Permalloy structure plays the role of an insulating barrier. TMR-like magnetoresistance is expected.[16]

(III) Ballistic junctions (BJ). Ballistic channels between two carbons encapsulated particles are connected to Co or Permalloy leads. BMR magnetoresistance is expected.

Four systematic characterizations are available at this nanoscopic scale, namely, the temperature dependence of the resistance $R(T)$, the magnetoresistance $R(H)$, the *I-V* characteristics and the time response of the resistance $R(t)$. The direct magnetic measurements (with usual magnetometers) are not available since the signals to be measured are of the order of 10^{-16} A m^2 (10^{-13} emu).

II. FABRICATION METHOD

Magnetic Co particles encapsulated in graphitic carbon shells are prepared by an arc discharge technique, and the structural and magnetic properties of the particles have been described in Ref. 17. Electron microscopy shows that the particles are mainly monocrystalline and covered by three to five graphitic shells. The mean diameter of the nanoparticles is 13.5 nm in the present case, with a dispersion of about 8 nm [Fig. 1(a)]. The magnetization of a single particle is about 1.8×10^{-18} A m^2. The blocking temperature is about 300 K, so that the particles do not have a superparamagnetic behavior in the temperature range of our experiments.

The nanowires are prepared in two main steps. First, the pores of a polycarbonate microfiltration membrane are filled with nanoparticles. The nanoparticles are dispersed in ethanol and driven into the pores by magnetophoretic deposition in a field of a 1 T magnet. Second, a metallic Co, or Permalloy matrix is electrodeposited in the pores, and a single nanowire is contacted by the method described in Refs. 19,18. The obtained nanowires are 6 μm long with a diameter of about 35 nm.

Transmission electron microscopy of the wires [Fig. 1(a)] reveals that the particles are densely compacted inside the pores. In a previous study[16] where carbon onions were used (particles composed by concentric carbon shells), we have shown that the GMR, or TMR-like magnetoresistance was

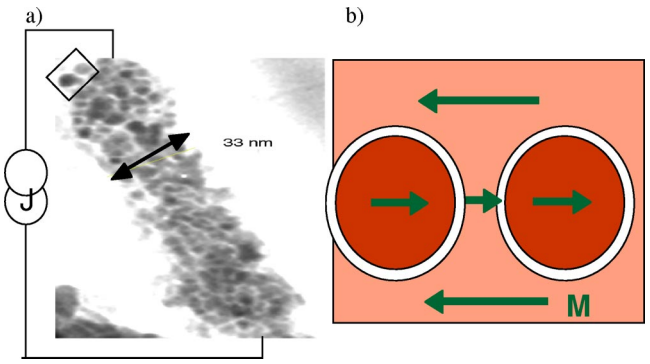

FIG. 1. (a) Transmission electron microscopy of a wire after dissolution of the membrane. The compacted nanoparticles are maintained together by the Co matrix. (b) Two neighboring particles are schematised with the magnetic configuration at zero external field, after saturation in a field perpendicular to the wire axis.

not due to the internal magnetic part of the particles, but either to surface scattering or due to the surrounding Co or permalloy magnetization. Consequently, the fact that particles are magnetized does not play a crucial role in the magnetoresistance in a first approach. This point will be discussed further below.

III. HUGE MAGNETORESISTANCE

The main feature of our nanocomposites is the colossal amplitude of the magnetoresistance measured at room temperature. The variations of the resistance are clearly related to the magnetization states. Different samples measured at room temperature are presented in Figs. 2–5.

The hysteresis are measured with a current of about 1 μA and with a magnetic field swept with a velocity of about 10 Oe/sec. The angle of the applied field is perpendicular to the wire axis (except in Fig. 5). The sign of the magnetoresistance depends on the state of the sample, which can be modified with temperature or high current injection (e.g., 1 mA pulse). At fixed temperature, the hysteresis loops are stable and can be repeated many times. However, as shown in Fig. 2, at $\sim\pm$4.5 kOe, a slow relaxation is responsible for the

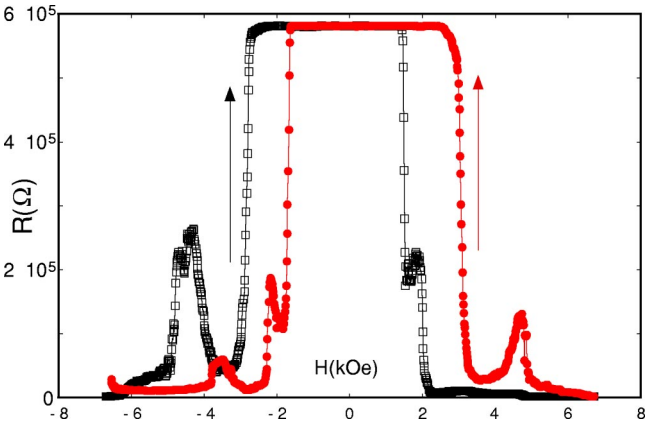

FIG. 2. Sample A. Magnetoresistance hysteresis loop with positive magnetoresistance. The magnetoresistance jumps by a factor 500 (about 50 000% MR).

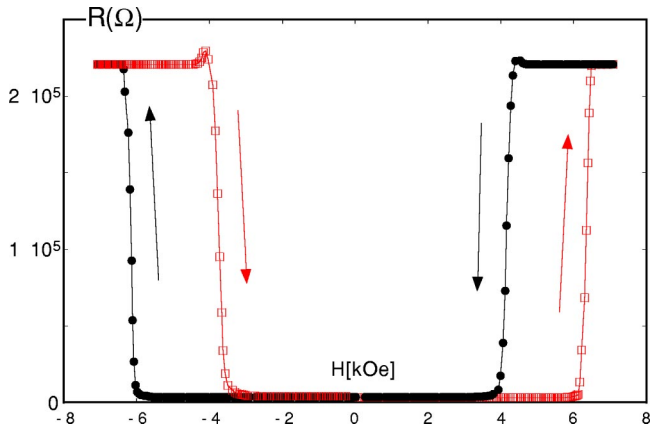

FIG. 3. Sample B. Magnetoresistance hysteresis loop with negative magnetoresistance. The magnetoresistance is about 10 000%.

typical humps observed (see below), which lead eventually to the decrease of the signal. In Fig. 4, the high field state at 14 800 Ω relaxes to the state at 17 000 Ω and the zero field state at 18 500 Ω relaxes to 22 500 Ω in a typical time of some few hours. It can also happen that the system freezes in a stable state, e.g., the higher resistance state of Fig. 2.

The *I-V* characteristics (non Ohmic) and the temperature dependence [jumps in the $R(T)$ profile] are discussed below, in the next section.

The second characteristic feature of such huge magnetoresistance, is the dependence to the angle of the applied field. Figure 5 shows that the sign of the magnetoresistance can be changed with 90° rotation of the magnetization.

We discuss now the possible role of magnetostriction as the cause of the large MR. It is known that the hcp c axis of Co electrodeposited in nanowires is often perpendicular to the wire axis.[20] Let us assume that it is the case for the sample shown in Fig. 5. If the hysteresis loop is performed with the applied field at 90° to the wire axis, the magnetization of the matrix is oriented also perpendicular to the wire axis at zero external field. Due to the strong dipole field, the carbon-encapsulated particles are oriented along the same axis and in the opposite direction. There is no magnetostric-

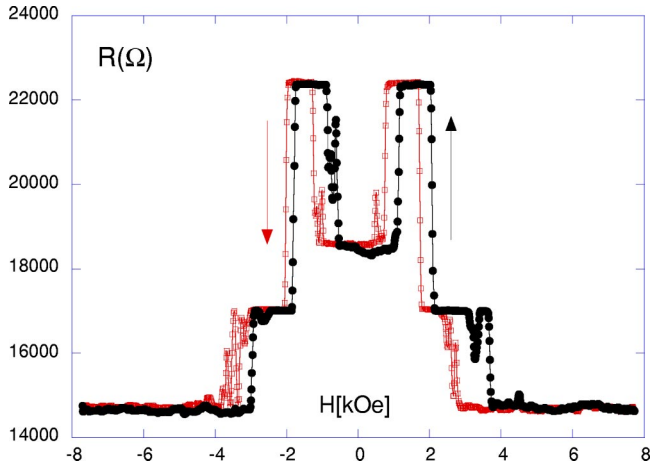

FIG. 4. Sample C. Magnetoresistance hysteresis loop. The magnetoresistance is about 52%.

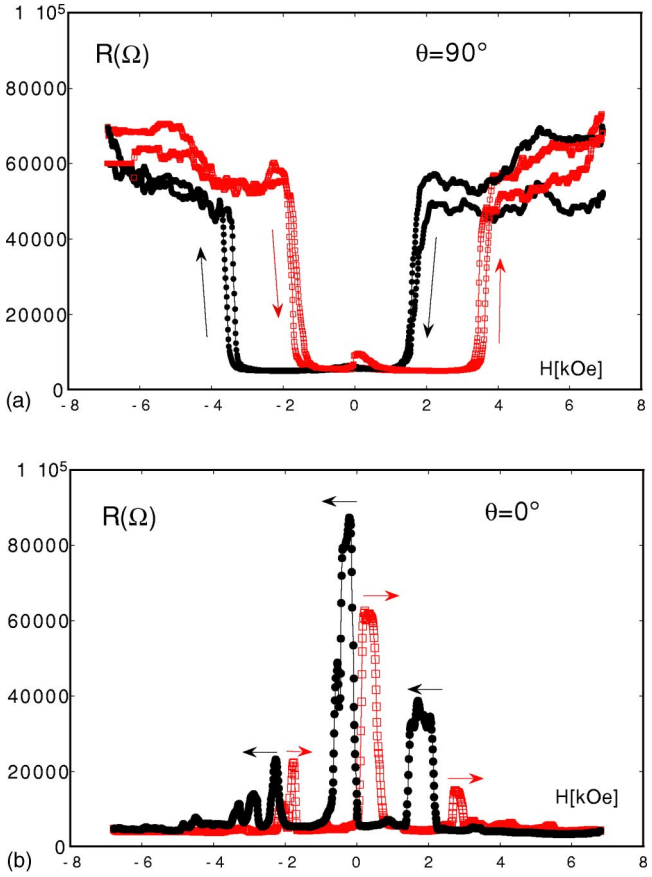

FIG. 5. Sample E. Magnetoresistance hysteresis loop at angle of the applied field (a) 90° (two successive loops) and (b) 0°, with respect to the wire axis. The magnetoresistance is about 1500%. The lower state is about 5 kΩ and the upper state is about 60 to 80 kΩ.

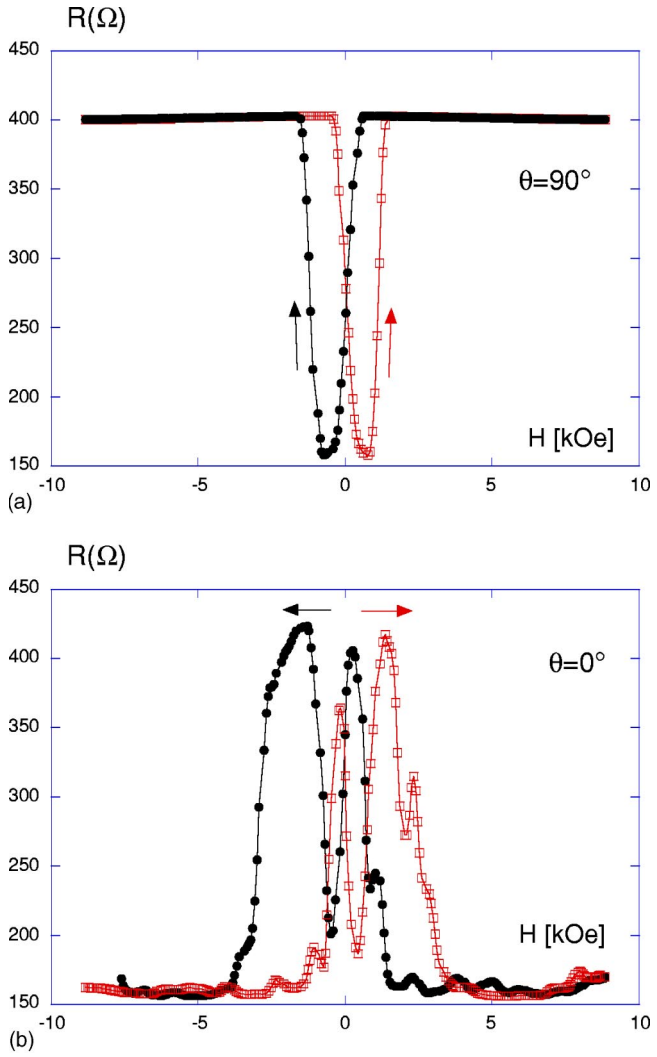

FIG. 6. Pore filled with permalloy matrix. Magnetoresistance hysteresis loop at angle of the applied field (a) 90° and (b) 0°, with respect to the wire axis. The magnetoresistance is about 250%.

tion in this case [see Fig. 1(b)]. On the other hand, if the hysteresis loop is performed with the applied field parallel to the wire axis, the magnetization of the matrix and the carbon encapsulated particles are oriented along the wire axis at zero external field. The magnetostriction is maximum in this case, with a relative constriction of -42×10^{-6}. However, it is not sufficient to account for a variation of a fraction of nm (five Co segments of 5 nm lead to a constriction of about 10^{-3} nm in the diameter, and 1000 segments leads to 0.2 nm constriction in the length). At least 1 nm displacement is necessary in order to account for a factor ten in the resistance. This corresponds to the obstruction or opening of one to ten conduction channels. A direct magnetostriction effect is hence not able to account for such signals.

Furthermore, the hypothesis of a magnetostrictive effect is invalidated by the same measurements performed with Permalloy samples. Figure 6 shows the magnetoresistance of a permalloy sample measured with the same protocol than that of the Co matrix sample shown in Fig. 5. The behavior is totally similar, with about 250% of magnetoresistance with a much smaller resistance (150 Ω in the lowest state). Taking into account that the magnetostriction is much smaller in permalloy than in Co, and that the crystallinity is very different (very small crystallites or amorphous structure), magnetostriction effects should not be observed, or at least be qualitatively different than that observed for Co matrix, which is not the case.

IV. RELAXATION AND JUMPS

The presence of relaxation between metastable states (Fig. 7) is the third main characteristic of such huge magnetoresistance. The system undergoes transitions from one state to the other at well-defined values of the external field. The slow relaxation has been measured in some of the samples, either by changing suddenly the field from saturation (8 kOe) down to zero, or by changing the angle of the applied saturation field from 45° to 130° [Fig. 5(b)].

The magnetization reversal of a single encapsulated Co nanoparticles below the blocking temperature is a sudden jump occurring at the subnanosecond time scale. The magnetization reversal of a full homogeneous Co (or permalloy) nanowire containing domain walls is also an event occurring within some tens of nanoseconds[21] (say some 100 ns in the

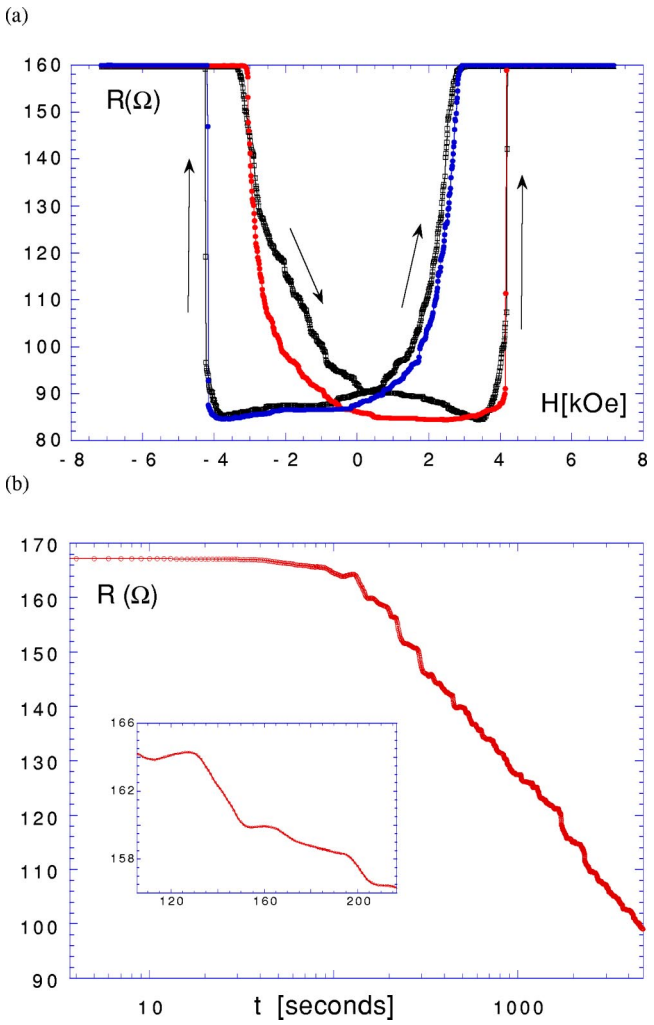

FIG. 7. Sample D. (a) Magnetoresistance hysteresis loop. The magnetoresistance is about 50%. (b) The same sample at 45° in a saturation field of 7 kOe. At $t=30$ s the sample was rotated from 45° to 130° initiating a logarithmic decay. Inset: typical structure with avalanches.

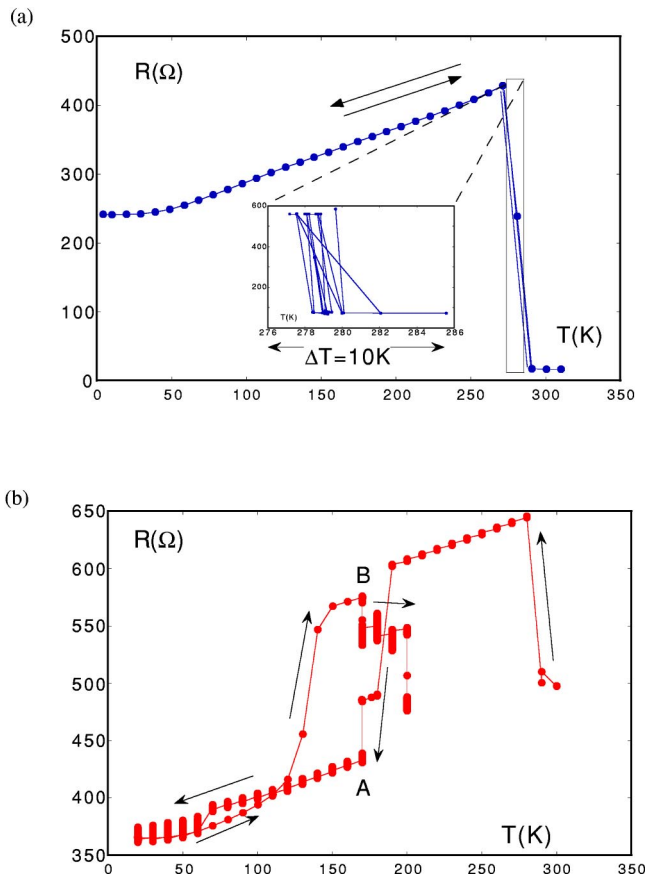

FIG. 8. Resistance as a function of the temperature for two samples (a) presented in section V and (b) in Fig. 9. Inset: The transition is performed by cycling the temperature within 10 K. (b) Hysteresis behavior of the resistance as a function of the temperature. The hysteresis is provoked by high current injection. The vertical bars shows the variation of resistance measured as a function of the current within ± 1 mA.

case of highly disordered wires). Consequently, the slow relaxation observed in Fig. 7(b) cannot be produced by the magnetic relaxation of the ferromagnetic matrix of the wire. If the magnetization reversal is averaged on an ensemble of ideally identical particles (or equivalently many times on the same particle) the relaxation is an exponential with a relaxation time τ_{sw} which is given by an Ahrrenius-like behavior (Neel-Brown-Coffey law[22]). If, furthermore, the potential energy barrier is given by a large distribution of such subensembles, the relaxation is close to a logarithmic behavior. These features are also valid in the case of structural relaxation of atoms, aggregate or dislocations. The relaxation of some hundreds of Co layers in the wire (studied, e.g., in Ref. 23) are also not sufficient to justify the logarithmic relaxation observed in Fig. 7(b). Furthermore, since the junction is localized between two nanoparticles, the signal is measured at this scale, and only some few particles are involved. Consequently, the relaxation is probably not due to magnetic relaxation, but to displacement of matter near the active junction.

The interpretation in terms of an elasticity effect is corroborated by an other characteristic behavior, observed on nearly all samples, which is the presence of sharp transitions of the resistance as a function of the temperature (that is, at constant magnetic configuration). The transition is evidenced by a high jump in the conductivity of a factor 2 to a factor 10 (Fig. 8). The most important feature of these jumps, which justify the term of transition, is that they are reversible or hysteretic. If the transition is performed by cycling the temperature over some few K below and above the transition, the transition temperature T_t measured by sweeping the temperature up and down is very stable (few K variations shown in the inset of in Fig. 8. A hysteresis can often be observed if the temperature variation is larger. The transition temperature T_t can be shifted by zero field cooling and field heating (ZFC/FC) loops. As shown in Fig. 8(b), the jump can also be produced by injecting high current density (few 100 μA). As shown in Fig. 7(b) the rotation of the external magnetic field can also responsible for the transition.

The transitions observed as a function of the temperature seems to be related to the one observed as a function of the magnetic field. Since the thermoelastic coefficient is rather

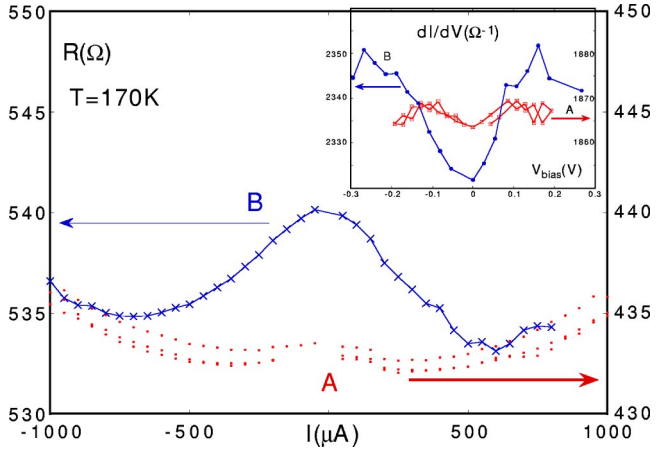

FIG. 9. Resistance as a function of the current at temperature 170 K before (A) and after (B) the hysteretic jump shown in Fig. 8(b).

high ($\alpha = 4 \times 10^{-6}$ K^{-1}) such behavior can be expected in the framework of the hypothesis of a magnetomechanical interpretation. The change occurs suddenly by discrete displacement of matter after a given amount of accumulated stress. Note that in the case of transitions due to temperature variations, the transition occurs without change of the magnetic configuration.

More information about the nature of this transition can be obtained by performing *I-V* characteristics (Fig. 9). The low resistance regime (e.g., below 100 Ω resistance) is apparently Ohmic. High resistance regime is strongly non-Ohmic, with all degrees in between.

The amplitude of the resistance, and the *I-V* characteristic (Fig. 8) is compatible with the hypothesis of tunnelling junction effects. Taking into account that there is no oxide in the wire (due to the reduction during electrodeposition), the non-Ohmic process occurs either through the carbon shells between the ferromagnetic matrix and the Co nanoparticles, either through holes in the structure of the Co matrix. It is possible to imagine some very small bridges, which can be broken reversibly, as in controllable break junction experiments (CBJ).[12,13,24] Unfortunately, this presence of holes or

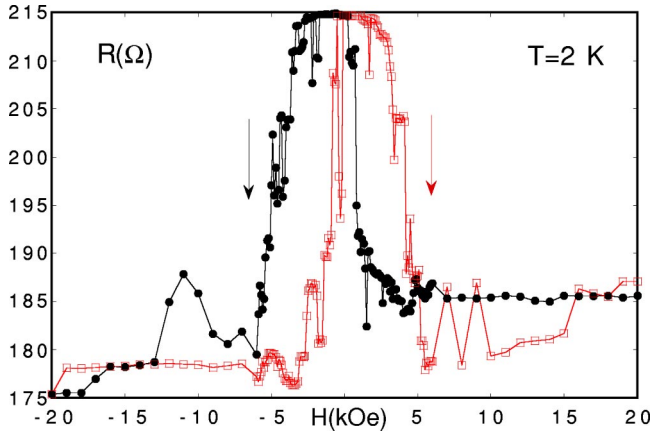

FIG. 10. Sample I. Magnetoresistance hysteresis loops measured at 2 K.

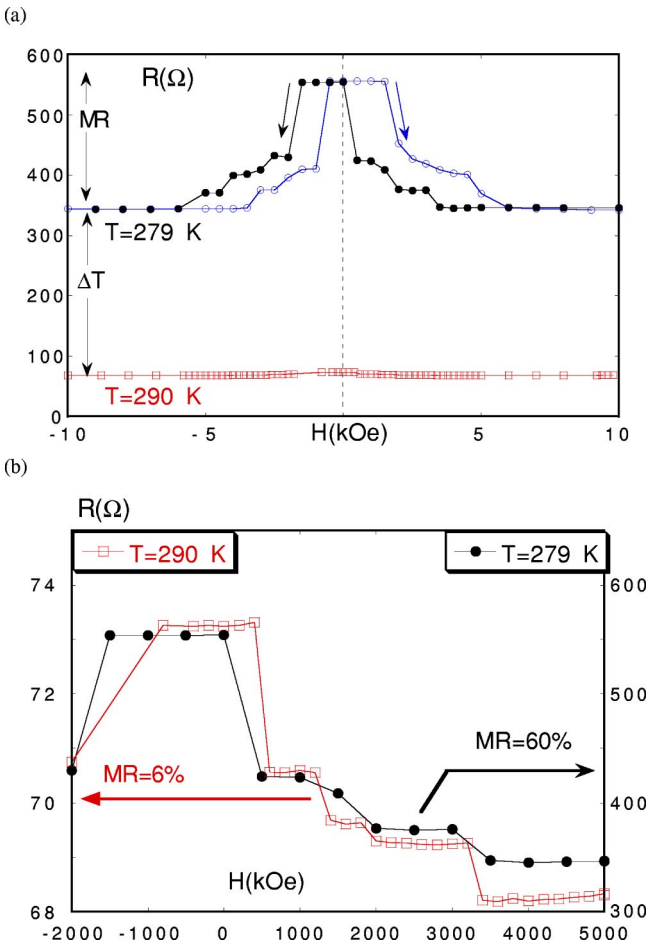

FIG. 11. Sample I. Magnetoresistance hysteresis loops measured at two different temperatures, above ($T = 290$ K) and below ($T = 279$ K) the transition. (a) Both hysteresis are plotted on the same scale. (b) The left scale corresponds to $T = 290$ K, and the right scale corresponds to the measure at $T = 279$ K.

bridges of the Co or permalloy matrix cannot be tested with transmission microscopy because the wires are destroyed precisely at such structural defaults during the dissolution of the membrane. Note, however, that the electrodeposition time of the Co (few seconds) is very different from that of permalloy (few hundred seconds), so that it is unlikely to have the same kind of holes in the two matrices.

These observations indicate that an indirect effect may be considered, where the magnetostatic forces between the particles or between particles and matrix leads to reversible displacement of matter in the system that obturates (or opens) some conduction channels. This movement of matter is probably also favored by electrostatic effects.

V. BALLISTIC MAGNETORESISTANCE

BMR signal can be measured only if nanomechanical effects can be ruled out. Such signals have been measured in some samples with small resistance. The small resistance guaranties that there is no tunnel barriers, and hence, no structural defects, like holes in the Co matrix. Figures 10 and 11 show magnetoresistance hysteresis loops measured at dif-

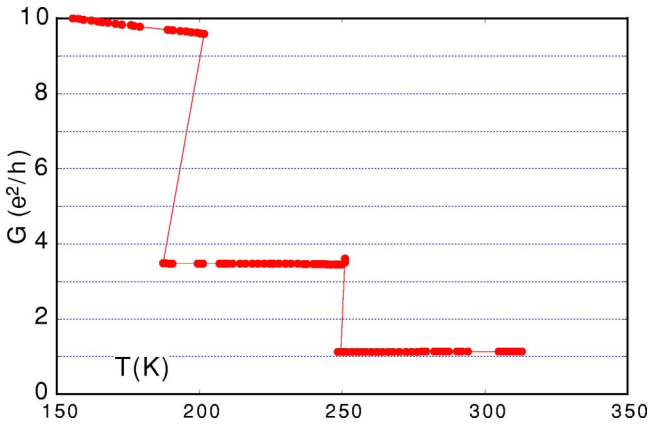

FIG. 12. Some jumps, similar to those observed in Figs. 2 –5are plotted as a function of the conductance quantization e^2/h.

ferent temperature. There are no relaxation effects here, the signal is perfectly stable and reproducible. The characteristic profile of the hysteresis is qualitatively different from that of the huge MR shown in the first section. The hysteresis is well defined, with a coercive field varying from about 5 to 2 kOe between 2 and 300 K, as expected for electrodeposited Co. The general behavior of the MR is similar to that of a trilayer pillar of Co/Cu/Co with 10 nm thicknesses of the layers, electrodeposited in a single wire.[25] This similarity suggests that dipole interaction, between two well-defined magnetic domains (e.g., the Co encapsulated in the carbon shells), is responsible for the signal. The maximum amplitude of the magnetoresistance measured in electrodeposited Co/Cu/Co trilayers was $\Delta R = 1\Omega$. In the present samples the magnetoresistance ranges from $\Delta R = 35\Omega$ (at 2 K) to $\Delta R = 250\Omega$ (at 279 K), leading to $\Delta R/R_{\min} = 20\%$ at 2 K, 25% at 25 K, 35% at 160 K, and 60% at 279 K. This surprising decrease of ΔR with increasing the temperature is not understood.

The most important feature of this type of MR (Fig. 11) is that the amplitude of the magnetoresistance is changing drastically, 6% above the transition temperature T_t, and 60% just below T_t, while the successive magnetic configurations observed in the hysteresis loop are unchanged. Figure 11(b) shows the superimposition of the two signals on different scales. We found that the change in the magnetoresistance is due to the change of the transport regime.

Evidence of the ballistic character of the conduction regime below T_t is shown in Fig. 12 (sample D). Note, however, that this quantization of the resistance at $R \approx 26\ k\Omega$ may be a coincidence since it is unlikely to have only one junction ballistic (or tunneling), and all the other junctions in series diffusive (i.e., negligibly small with respect to 13 kΩ). The resistance of the other junctions in series can be seen at $4G_0$ and at 10 or $11G_0$. Note that, as already observed (and expected),[26] the conductance quantization under field is $G_0/2 = e^2/h$ and not $G_0 = 2e^2/h$ as in usual metallic structures.

VI. CONCLUSION

Circuits of nanoscopic junctions with constrained magnetic domain walls have been obtained by magnetophoretic deposition of nanoparticles in porous membranes, followed by electrodeposition of Co or permalloy matrix. Magnetic domain walls, constrained at a typical scale of some few nanometers are induced between the particles by the strong dipole interactions and pinning centers. Very high magnetoresistance signals related to the magnetic configurations have been measured systematically in samples with high resistance. The amplitude of the signals, the relaxation processes, and the dependence of the angle of the applied field tend to show that this effect is due to reversible displacement of matter (i.e., elasticity) close to conduction channels or tunnelling barriers. The elasticity is not produced by magnetostriction. The resistance as a function of the temperature shows that a similar signal appears initiated by thermoelastic effect. Magnetostatic forces (strong dipole and multipole interactions) and electrostatic forces must be invoked in order to account for the observed effects. This nano-mechanical aspect of the samples must be studied further as such in forthcoming measurements.

On the other hand, the strong nanomechanical effects can be ruled-out in some samples (e.g. in samples with small resistance, and no relaxation effects, i.e., without tunneling barrier). A magnetoresistance signal of some tens of percents (60% close to room temperature), has been observed. This signal is very similar to that of usual CPP giant magnetoresistance measured, e.g., in Co/Cu/Co pillars, except the too high amplitude for nanoscopic junctions. Some evidence shows that the appearance of the giant magnetoresistance is related to a change in the conduction regime from diffusive to ballistic. This seems to indicate that the observed signals are due to ballistic magnetoresistance.

ACKNOWLEDGMENTS

We are grateful to the Center Interdépartemental de Microscopie Electronique of EPFL (CIME-EPFL) for access to electron microscopy facilities. It is also a pleasure to thank M. Coey and S. Parkin for interesting discussions. This work was supported by Grant No. 5812.1 of the Swiss program TOP NANO 21.

*Present address: LSI, Ecole Polytechnique, 91128 Palaiseau Cedex, France. Email address: wegrowe@hp1sesi.polytechnique.fr

[1] G.A. Prinz, Science **282**, 1660 (1998).

[2] C. Joachim, J.C. Gimzewski, and A. Aviram, Nature (London) **408**, 541 (2000).

[3] J. S. Moodera, L.R. Kinder, T. M. Kinder, T. M. Wing, and R. Meservey, Phys. Rev. Lett. **74**, 3273 (1995).

[4] A. Gerber, Physica B **280**, 331 (2000); A. Milner, A. Gerber, B. Groisman, M. Karpovsky, and A. Gladkikh, Phys. Rev. Lett. **76**, 475 (1996); A. Gerber, A. Milner, B. Groisman, M. Karpovsky, A. Gladkikh, and A. Sulpice, Phys. Rev. B **55**, 6446 (1997).

[5] B. Doudin, G. Redmond, S. W. Gilbert, and J.-Ph. Ansermet, Phys. Rev. Lett. **79**, 933 (1997).

[6] M. N. Baibich, J. M. Broto, A. Fert, F. Nguyen Van Dau, and F.

Petroff, Phys. Rev. Lett. **61**, 2472 (1988).
[7] G. Binash, P. Grünberg, F. Saurenbach, and W. Zinn, Phys. Rev. B **39**, 4828 (1989).
[8] A. E. Berkowitz, J. R. Mitchell, M. J. Carey, A. P. Young, S. Zhang, and G. Thomas, Phys. Rev. Lett. **68**, 3745 (1992).
[9] J. Q. Xiao, J. S. Jiang, and C. L. Chien, Phys. Rev. Lett. **68**, 3749 (1992).
[10] P. Bruno, Phys. Rev. Lett. **83**, 2425 (1999).
[11] J. M. Coey, L. Berger, and Y. Labaye, Phys. Rev. B **64**, 020407 (2001).
[12] N. Garcia, M. Munoz, and Y. W. Zhao, Phys. Rev. Lett. **82**, 2923 (1999); N. Garcia, M. Munoz, G. G. Qian, H. Rohrer, I. G. Saveliev, and Y. W. Zhao, Appl. Phys. Lett. **79**, 4550 (2001); N. Garcia, M. Munoz, G. G. Qian, and I. G. Saveliev, *ibid.* **80**, 1785 (2002).
[13] J. J. Versluijs, M. A. Bari, and J. M. D. Coey, Phys. Rev. Lett. **87**, 026601 (2001).
[14] H. D. Chopra and S. Z. Hua, Phys. Rev. B **66**, 020403(R) (2002).
[15] M. Viret, S. Berger, M. Gabureac, F. Ott, D. Olligs, I. Petej, J. F. Gregg, C. Fermon, G. Francinet, and G. Le Goff, Phys. Rev. B **66**, 220401(R) (2002).
[16] J.-E. Wegrowe, A. Sallin, A. Fabian, A. Comment, J.-M. Bonard, and J.-Ph. Ansermet, Phys. Rev. B **65**, 012407 (2001).
[17] J-M. Bonard, S. Seraphin, J-E. Wegrowe, T. Stockli, J. Jiao, and A. Chatelain, Chem. Phys. Lett. **343**, 251 (2001).
[18] J.-E. Wegrowe, S. E. Gilbert, V. Scarani, D. Kelly, B. Doudin, and J.-Ph. Ansermet, IEEE Trans. Magn. **34**, 903 (1998).
[19] J.-E. Wegrowe, D. Kelly, A. Franck, S. E. Gilbert, and J.-Ph. Ansermet, Phys. Rev. Lett. **82**, 3681 (1999).
[20] V. Scarani, B. Doudin, and J.-Ph. Ansermet, J. Magn. Magn. Mater. **205**, 241 (1999).
[21] Ph. Guittienne, J.-E. Wegrowe, D. Kelly, and J.-Ph. Ansermet, IEEE Trans. Magn. **Mag-37**, 2126 (2001).
[22] W. T. Coffey, D. S. F. Crothers, J. L. Dormann, Yu. P. Kalmykov, E. C. Kennedy, and W. Wernsdorfer, Phys. Rev. Lett. **80**, 5655 (1998).
[23] B. Doudin, J.-E. Wegrowe, S. E. Gilbert, V. Scarani, D. Kelly, J. P. Meier, and J.-Ph. Ansermet, IEEE Trans. Magn. **34**, 968 (1998).
[24] J.M. van Ruitenbeek, in *Metal Clusters on Surfaces: Structure, Quantum Properties, Physical Chemistry*, edited by K.H. Meiwes-Broer (Springer-Verlag, Heidelberg, 2000), pp. 175–210.
[25] J.-E. Wegrowe, A. Fabian, X. Hoffer, Ph. Guittienne, D. Kelly, E. Olive, and J.-Ph. Ansermet, Appl. Phys. Lett. **80**, 3775 (2002).
[26] Teruo Ono, Yutaka Ooka, Hideeki Miyajima, and Yoshichika Otani, Appl. Phys. Lett. **75**, 1622 (1999).